Higgs physics results at ATLAS

Rhys Owen[1] on behalf of the ATLAS Collaboration
STFC - Rutherford Appleton Laboratory[1]
Moriond QCD 28th March 2021

ATLAS EXPERIMENT

Science and Technology Facilities Council

ATLAS Higgs results presented in this talk

Search/measurement of rare Standard Model (SM) processes

- Focus of this talk, rare (but within reach) processes which might give more insight into the nature of the 125 GeV Higgs boson
- Latest SM Higgs boson results from ATLAS

Search for ultra-rare or Beyond Standard Model (BSM) processes

- Dedicated talk on ATLAS search program later in the week from Stefania Xella
- Some details here of SM Higgs boson decays which are outside of our reach without BSM enhancement
- Search for di-Higgs production to measure Higgs self coupling
- Latest BSM Higgs boson results from ATLAS

Also from ATLAS there are a wide range of precision differential measurements and charge parity (CP) studies

- See talk from Sébastien Rettie later in this session

ATLAS LHC Run-2 Dataset

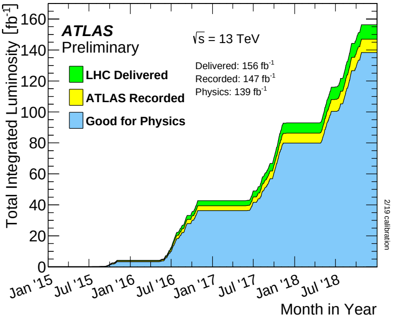

ATLAS pp Run-2: July 2015 – October 2018

Inner Tracker			Calorimeters		Muon Spectrometer				Magnets	
Pixel	SCT	TRT	LAr	Tile	MDT	RPC	CSC	TGC	Solenoid	Toroid
99.5	99.9	99.7	99.6	99.7	99.8	99.6	100	100	99.8	98.8

Good for physics: 95.6% (139 fb^{-1})

Luminosity weighted relative detector uptime and good data quality efficiencies (in %) during stable beam in pp collision physics runs with 25 ns bunch-spacing at $\sqrt{s}$=13 TeV for the full Run-2 period (between July 2015 – October 2018), corresponding to a delivered integrated luminosity of 153 fb^{-1} and a recorded integrated luminosity of 146 fb^{-1}. Runs with specialized physics goals are not included. Dedicated luminosity calibration activities during LHC fills used 0.6% of recorded data in 2018 and are included in the inefficiency. Trigger-specific data quality problems (0.4% inefficiency at Level-1) are included in the overall inefficiency. When the stable beam flag is raised, the tracking detectors undergo a so-called "warm start", which includes a ramp of the high-voltage and turning on the pre-amplifiers for the Pixel system. The inefficiency due to this, as well as the DAQ inefficiency, are not included in the table above, but accounted for in the ATLAS data taking efficiency.

ATLAS profited from the consistent performance of the LHC in Run-2

- High data recording and quality efficiency mean that we now have a large dataset filled with candidate Higgs boson decays to study
- Statistical uncertainty is still dominates many analyses
- All analyses discussed here using the full data set
- Run-2 luminosity of 139 fb^{-1} represents a large increase over the 24.8 fb^{-1} from Run-1

VBF $H \to b\bar{b}$: Motivation

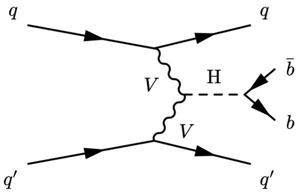

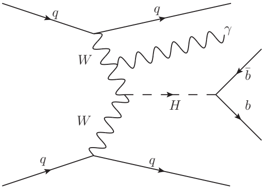

$H \to b\bar{b}$ provides the biggest SM branching ratio but also suffers from large QCD backgrounds

- VBF production is used to reduce the backgrounds
- The two analyses feature different techniques to identify this signal
- The first approach selects events directly with two b-tagged jets and two from the VBF
- The second approach uses an additional initial state radiation photon to provide a trigger and reduce the multijet background

arXiv:2011.08280 arXiv:2010.13651

VBF $H \to b\bar{b}$: Adversarial Neural Network

Adversarial Neural Network (ANN) used to select signal events

- Network trained on event kinematics
- The "Adversary" penalises the training of the classifier if it is sensitive to $m_{b\bar{b}}$
- Signal taken from MC but background from $m_{b\bar{b}}$ side bands
- Analysis is split into forward and central channels and 5 classifier regions

Background shape then independent of ANN score

- This means the shape parameters can be fit in the Low score High statistics region for each channel

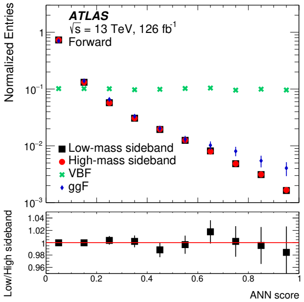

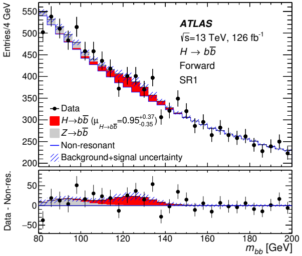

arXiv:2011.08280

VBF $H \to b\bar{b}\gamma$

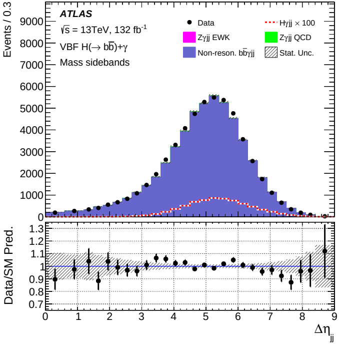

Events are selected by a dedicated trigger

- A single photon at level 1 then 4 jets or 3 jets and a b-jet in the higher level trigger
- A BDT is trained on event kinematics using MC samples for signal and background
- The non-resonant background sample used in the training is re-weighted using data side-bands to improve the agreement

Three signal regions defined based on BDT output

- Expected yield varies by an order of magnitude between Low and High BDT regions.

arXiv:2010.13651

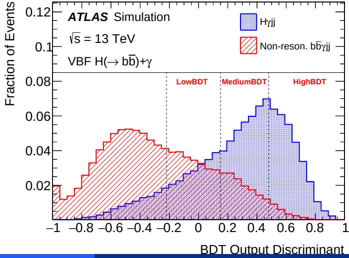

VBF $H \to b\bar{b}$: Results

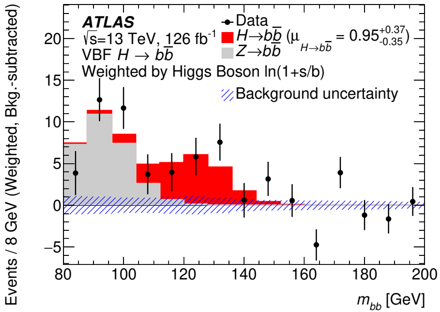

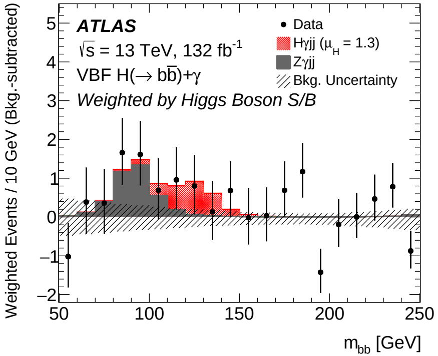

The combined signal strength is $\mu_{VBF} = 0.99^{+0.30}_{-0.30}(Stat.)^{+0.18}_{-0.16}(Syst.)$

- Corresponds to an observed (expected) significance of 2.9(2.9)σ
- Very close to sensitivity for evidence in this channel

arXiv:2011.08280 arXiv:2010.13651

Evidence for $H \to \ell\ell\gamma$: Motivation

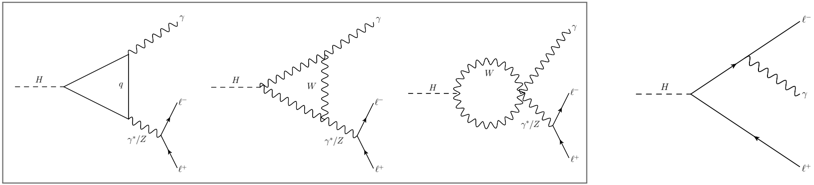

$H \to \ell\ell\gamma$ final state provides a probe of possible exotic couplings from extensions to the SM

- This analysis considered $m_{\ell\ell} < 30$ GeV
- Dominated by $\gamma^{\star}$ contribution
- Small SM branching ratio but three particle decays can provide information on the CP nature of the Higgs Boson in the future

arXiv:2103.10322

Evidence for $H \to \ell\ell\gamma$: Events

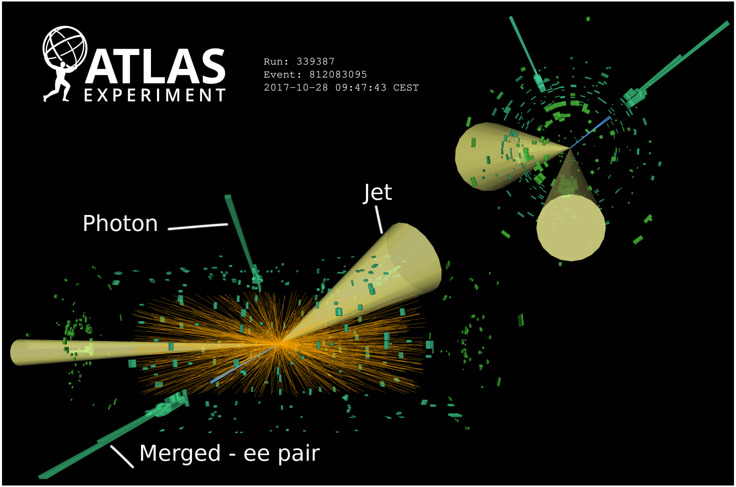

$\ell\ell\gamma$ events are selected from the full Run-2 139 fb^{-1} dataset

- A dedicated merged–*ee* reconstruction is used to recover efficiency where electron energy deposits overlap, $> 3\times$ increase in acceptance for low m_{ee}
- Event displayed from merged–*ee* VBF Category arXiv:2103.10322

Evidence for $H \to \ell\ell\gamma$: Signal and Background Modelling

Events are categorised based on lepton type and the event kinematics

- Resulting in 9 orthogonal categories ($\mu\mu$,*ee*,merged–*ee*) x (VBF-enriched, High P_{Tt}, Low P_{Tt})
- $P_{Tt} = |\vec{P}_T^{\ell\ell\gamma} \times \hat{t}|, \hat{t} = (\vec{P}_T^{\ell\ell} - \vec{P}_T^{\gamma})/|\vec{P}_T^{\ell\ell} - \vec{P}_T^{\gamma}|$

Signal parametrised from Double-Sided Crystal Ball fit to Monte-Carlo

Background parametrisation is selected per category to minimise bias

- Background components from non-resonant $\ell\ell\gamma$ production as well as $\ell\ell +$ jets and $\gamma +$ jets.
- Templates are created from MC (Non-resonant) or data control regions (fakes) and used to test the parametrisation

Signal strength determined from simultaneous fit to categories

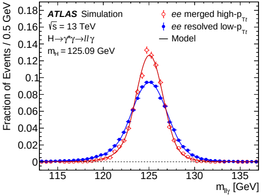

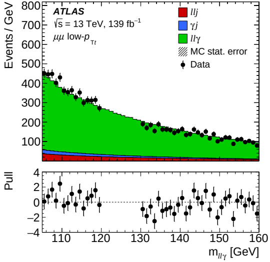

arXiv:2103.10322

Evidence for $H \to \ell\ell\gamma$: Results

Best-fit of the signal strength parameter is $\mu = 1.5 \pm 0.5$

- This represents a significance of 3.2 σ over the background only hypothesis (2.1 σ expected)
- Final uncertainty driven by the low statistics

First evidence of Higgs boson decays to this final state

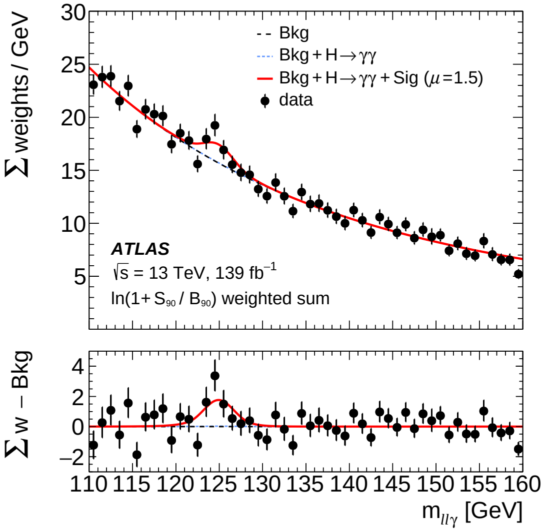

arXiv:2103.10322

Search for $H \to Z(\to \ell\ell)\gamma$: Events

$Z\gamma$ events are selected from the full Run-2 139 fb^{-1} dataset

- Similar lepton requirements to $\ell\ell\gamma$ but $|92.1 - m_{\ell\ell}| < 10$ GeV and no merged–ee necessary
- $Z \to \mu\mu$ mass resolution is improved by correcting for co-linear final state radiation photons identified in the calorimeter
- Relative $P_T^\gamma / m_{Z\gamma} > 0.12$

Events are further categorised based on lepton type and the event kinematics

- VBF events selected by BDT
- $P_T^\gamma / m_{Z\gamma} > 0.4$ form a high relative P_T category
- Remaining events are split by $P_{Tt} > 40$ GeV and lepton flavour
- Resulting in 6 orthogonal categories

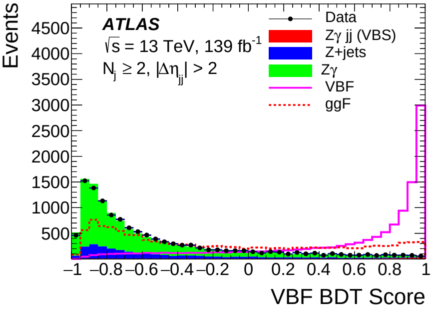

Phys. Lett. B 809 (2020) 135754

Search for $H \to Z(\to \ell\ell)\gamma$: Results

Final fit combines signal and background from the different categories

- Signal parametrised from Double-Sided Crystal Ball fit to Monte-Carlo
- Background parametrisation is selected per category to minimise bias

95% CL limit on the signal strength is 3.6 times the SM prediction

- Best-fit of the signal strength parameter is $\mu = 2.0 \pm 0.9(stat.)^{+0.4}_{-0.3}(syst.)$
- Expected limits were 1.7 or 2.6 for a null hypotheses excluding or including the SM Higgs production
- More data needed for conclusive evidence in this channel

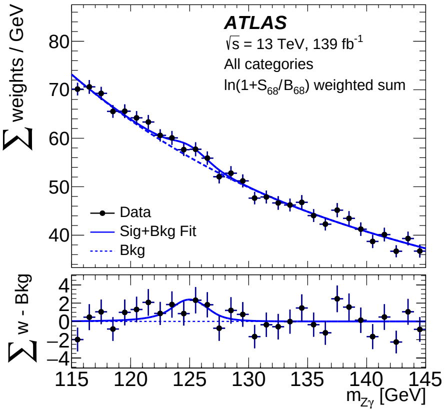

Phys. Lett. B 809 (2020) 135754

Search for $HH \to b\bar{b}\gamma\gamma$: Motivation

New Result

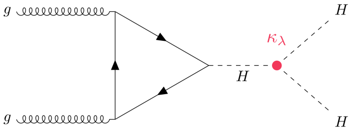

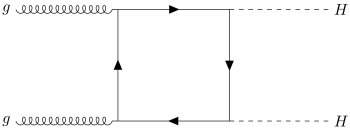

$HH \to b\bar{b}\gamma\gamma$ provides updated limits on di-Higgs production

- Rare process in the SM with $\sigma_{HH}(ggF) = 31.05$ fb at 13TeV in NNLO FTapprox
- Clean $H \to \gamma\gamma$ system for trigger and selection
- $H \to b\bar{b}$ for the large SM branching ratio
- New constraints on the signal strength ($\sigma_{HH}/\sigma_{HH}^{\text{SM}}$) and on the Higgs boson self-coupling modifier $\kappa_\lambda = \lambda_{HHH}/\lambda_{HHH}^{\text{SM}}$ that affects the interference pattern between the possible production diagrams.
- VBF production also included but not specifically targeted
- Also a search for resonant BSM physics with $X \to HH \to b\bar{b}\gamma\gamma$

ATLAS-CONF-2021-016

$HH \rightarrow b\bar{b}\gamma\gamma$: Events

New Result

Event selection

- Triggered by the presence of two photons
- 105 GeV $< m_{\gamma\gamma} <$ 160 GeV
- Required to have fewer than 6 central jets
- Exactly two b-tagged jets (77% efficiency)
- Veto events containing an electron or muon

Modified invariant mass $m^{\star}_{b\bar{b}\gamma\gamma}$ calculated

- $m^{\star}_{b\bar{b}\gamma\gamma} = m_{b\bar{b}\gamma\gamma} - m_{b\bar{b}} - m_{\gamma\gamma} + 250$ GeV
- Improves mass resolution especially for resonant HH searches
- Provides cancellation of experimental resolution effects
- Low and high mass categories provide enhanced sensitivity to κ_λ
- $m^{\star}_{b\bar{b}\gamma\gamma} < 350$ GeV defined as low mass
  $m^{\star}_{b\bar{b}\gamma\gamma} > 350$ GeV as high mass

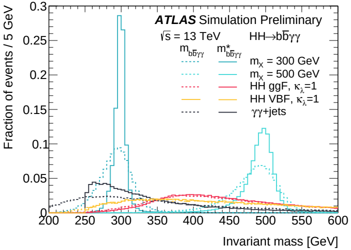

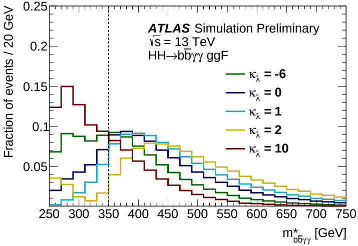

ATLAS-CONF-2021-016

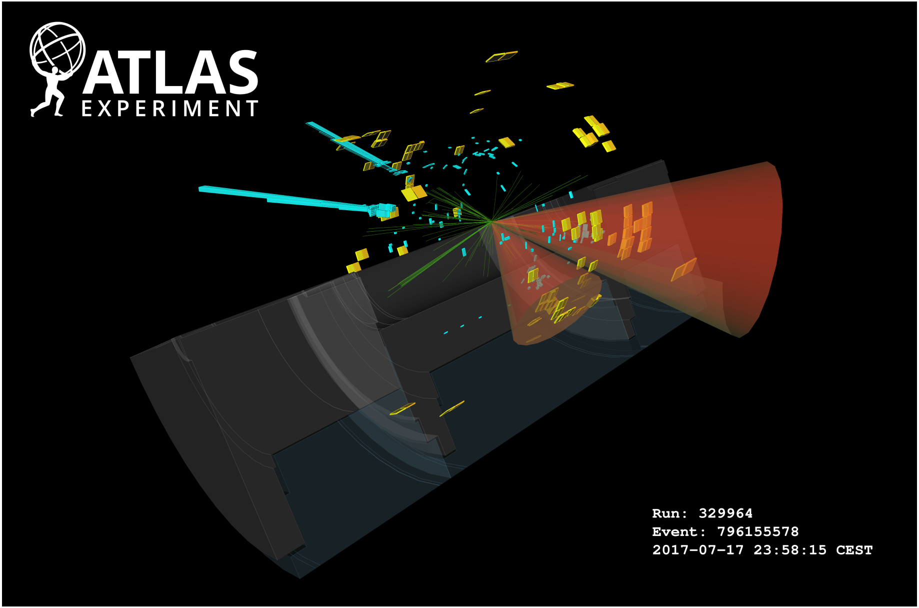

ATLAS-CONF-2021-016

$HH \to b\bar{b}\gamma\gamma$: Results

New Result

Signal regions defined using BDT score and $m^{\star}_{b\bar{b}\gamma\gamma}$ categories

- BDT trained on photon, jet and missing transverse energy variables to reject $\gamma\gamma$ and single Higgs backgrounds

$m_{\gamma\gamma}$ used as final discriminant in the fit

- Signal and single Higgs background parametrised as Double-Sided Crystal Ball for both *ggF* and VBF production modes
- Continuum $\gamma\gamma$ background parametrised by exponential

Limits set on *HH* production

- 95% CL limits on *HH* production observed (expected) at 4.1 (5.5) times the SM prediction
- 5× improvement over previous result and current best available limits
- 95% confidence interval on κ_λ of $[-1.5, 6.7]$ ($[-2.4, 7.7]$)

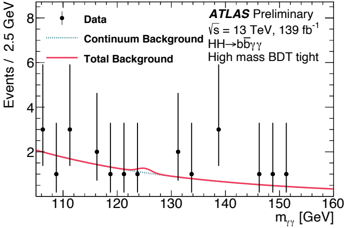

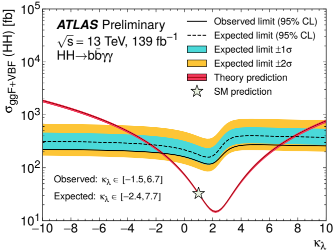

ATLAS-CONF-2021-016

$X \to HH \to b\bar{b}\gamma\gamma$: Results

New Result

Signal regions defined using BDT score and $m^{\star}_{b\bar{b}\gamma\gamma}$ categories

- $m^{\star}_{b\bar{b}\gamma\gamma} \pm 2\sigma$ window around each mass point
- Two BDTs are trained to discriminate against $\gamma\gamma$ and single Higgs backgrounds
- For each mass-point a requirement is placed on the BDT score to maximise the significance

Limits set on $\sigma(X \to HH)$ for a wide range of m_X

- $m_{\gamma\gamma}$ used as final discriminant in the fit
- In this case SM HH production included as a background

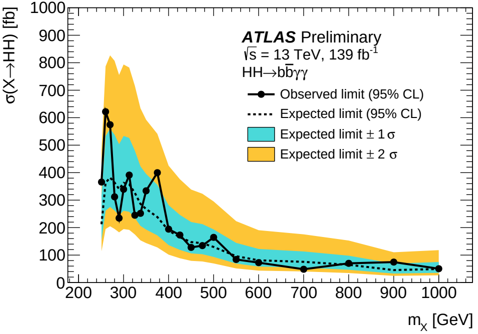

ATLAS-CONF-2021-016

Search for heavy resonances decaying to a pair of photons

Extension of SM $H \rightarrow \gamma\gamma$ studied to higher masses

- Selecting two isolated photons passing tight identification requirements
- $m_{\gamma\gamma} > 150$ GeV
- spin-0 and spin-2 resonances considered

No significant excess is observed over the SM background

- 95% Confidence level limits set on the models using the CL_s method
- Limits range from 12.5 to 0.03 fb for spin-0 narrow width approximation
- For spin-2 with coupling $k/\bar{M}_{P1} = 0.1$ the limits range from 3.2 to 0.04 fb and the RS1 graviton is excluded for masses below 4.5 TeV

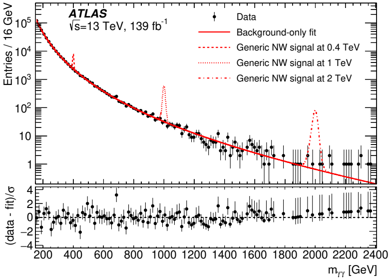

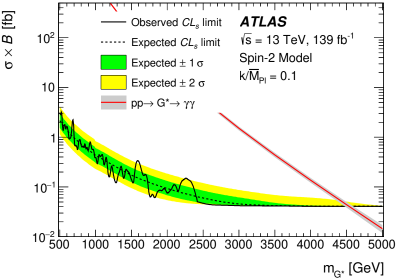

arXiv:2102.13405

Conclusions

ATLAS Run-2 Dataset allows us to probe ever more subtle Higgs boson interactions

- First evidence for non-resonant $H \to \ell\ell\gamma$
- Improved limits on di-Higgs production
- New measurements of VBF production in the $b\bar{b}$ decay channel
- These analyses compliment differential measurements made in other channels

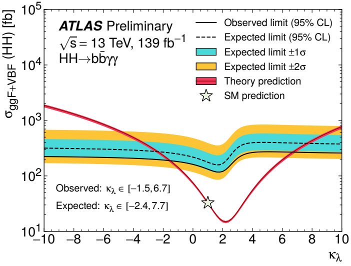

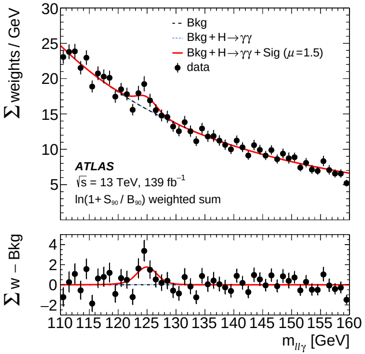

Backup

Evidence for $H \rightarrow \ell\ell\gamma$: Selection

Category	Events	S_{90}	B_{90}^{N}	$B_{H\rightarrow\gamma\gamma}$	f_{90} [%]	Z_{90}
ee resolved VBF-enriched	10	0.4	1.6	0.009	20	0.3
ee merged VBF-enriched	15	0.8	2.0	0.07	27	0.5
$\mu\mu$ VBF-enriched	33	1.3	5.9	–	18	0.5
ee resolved high-$p_{\mathrm{T}t}$	86	1.1	12	0.02	9	0.3
ee merged high-$p_{\mathrm{T}t}$	162	2.5	18	0.2	12	0.6
$\mu\mu$ high-$p_{\mathrm{T}t}$	210	4.0	34	–	11	0.7
ee resolved low-$p_{\mathrm{T}t}$	3713	22	729	0.5	2.9	0.8
ee merged low-$p_{\mathrm{T}t}$	5103	29	942	2	3.0	1.0
$\mu\mu$ low-$p_{\mathrm{T}t}$	9813	61	1750	–	3.4	1.4

arXiv:2103.10322

Evidence for $H \to \ell\ell\gamma$: Systematic Breakdown

<table>
<tr><th>Uncertainty source</th><th>μ</th><th>$\sigma \times \mathcal{B}$</th></tr>
<tr><td>Spurious Signal</td><td colspan="2">6.1</td></tr>
<tr><td>$\mathcal{B}(H \to \ell\ell\gamma)$</td><td>5.8</td><td>–</td></tr>
<tr><td>QCD scale</td><td>4.7</td><td>1.1</td></tr>
<tr><td>ℓ, γ, jets</td><td colspan="2">4.0</td></tr>
<tr><td>PDF</td><td>2.3</td><td>0.9</td></tr>
<tr><td>Luminosity</td><td colspan="2">1.7</td></tr>
<tr><td>Pile-up</td><td colspan="2">1.7</td></tr>
<tr><td>Minor prod. modes</td><td colspan="2">0.8</td></tr>
<tr><td>$H \to \gamma\gamma$ background</td><td colspan="2">0.7</td></tr>
<tr><td>Parton Shower</td><td colspan="2">0.3</td></tr>
<tr><td>Total systematic</td><td>11</td><td>7.9</td></tr>
<tr><td>Statistical</td><td colspan="2">31</td></tr>
<tr><td>Total</td><td>33</td><td>32</td></tr>
</table>

Search for $H \rightarrow Z(\rightarrow \ell\ell)\gamma$: Selection

Category	Events	S_{68}	B_{68}	w_{68} [GeV]	S_{68}/B_{68} $[10^{-2}]$	$S_{68}/\sqrt{S_{68}+B_{68}}$
VBF-enriched	194	2.7	18.7	3.7	14.3	0.58
High relative p_{T}	2276	7.6	112.8	3.7	6.7	0.69
High $p_{\mathrm{T}t}$ ee	5567	9.9	444.0	3.8	2.2	0.46
Low $p_{\mathrm{T}t}$ ee	76 679	34.5	6654.1	4.1	0.5	0.42
High $p_{\mathrm{T}t}$ $\mu\mu$	6979	12.0	610.8	3.9	2.0	0.48
Low $p_{\mathrm{T}t}$ $\mu\mu$	100 876	43.5	8861.5	4.0	0.5	0.46
Inclusive	192 571	110.2	16 701.9	4.0	0.7	0.85

Phys. Lett. B 809 (2020) 135754

Search for $H \to Z(\to \ell\ell)\gamma$: Systematic Breakdown

Sources	$H \to Z\gamma$
Luminosity [%]	
Luminosity	1.7
Signal efficiency [%]	
Modelling of pile-up interactions	0.0–0.2
Photon identification efficiency	0.8–1.8
Photon isolation efficiency	0.7–1.9
Electron identification efficiency	0.0–2.3
Electron isolation efficiency	0.0–0.1
Electron reconstruction efficiency	0.0–0.5
Electron trigger efficiency	0.0–0.1
Muon selection efficiency	0.0–0.6
Muon trigger efficiency	0.0–1.6
Jet energy scale	0.0–3.5
Jet resolution	0.0–15
Jet pile-up	0.0–7.5
Jet flavor	0.0–11
Signal modelling on σ_{CB} [%]	
Electron and photon energy resolution	0.5–3.4
Muon – Inner detector resolution	0.0–1.2
Muon – Muon spectrometer resolution	0.0–3.4
Signal modelling on μ_{CB} [%]	
Electron and photon energy scale	0.09–0.15
Muon momentum scale	0.0–0.03
Higgs boson mass measurement	0.19
Background modelling [number of spurious signal events]	
Spurious signal	1.5–39

Phys. Lett. B 809 (2020) 135754

Sources	
Total cross-section and efficiency [%]	
ggF Underlying event	1.3
perturbative order	4.7–9.6
PDF and α_s	1.8–2.8
$B(H \to Z\gamma)$	5.7
Total (total cross-section and efficiency)	7.5–11
Category acceptance [%]	
ggF Underlying event	0.1–11
ggF H p_T perturbative order	0.3–0.4
ggF in VBF-enriched category	37
ggF in high relative p_T category	21
ggF in other categories	10–15
Other production modes	1.0–15
PDF and α_s	0.4–3.5
Total (category acceptance)	11–37

Search for $HH \to bb\gamma\gamma$: non-resonant BDT

Variable	Definition
Photon-related kinematic variables	
$p_{\mathrm{T}}/m_{\gamma\gamma}$	Transverse momentum of the two photons scaled by their invariant mass $m_{\gamma\gamma}$
η and ϕ	Pseudo-rapidity and azimuthal angle of the leading and sub-leading photon
Jet-related kinematic variables	
b-tag status	Highest fixed b-tag working point that the jet passes
p_{T}, η and ϕ	Transverse momentum, pseudo-rapidity and azimuthal angle of the two jets with the highest b-tagging score
$p_{\mathrm{T}}^{b\bar{b}}$, $\eta_{b\bar{b}}$ and $\phi_{b\bar{b}}$	Transverse momentum, pseudo-rapidity and azimuthal angle of b-tagged jets system
$m_{b\bar{b}}$	Invariant mass built with the two jets with the highest b-tagging score
H_{T}	Scalar sum of the p_{T} of the jets in the event
Single topness	For the definition, see Eq. (1)
Missing transverse momentum-related variables	
$E_{\mathrm{T}}^{\mathrm{miss}}$ and ϕ^{miss}	Missing transverse momentum and its azimuthal angle

ATLAS-CONF-2021-016

Search for $HH \to bb\gamma\gamma$: resonant BDT

Variable	Definition
Photon-related kinematic variables	
$p_{\mathrm{T}}^{\gamma\gamma}$, $y^{\gamma\gamma}$	Transverse momentum and rapidity of the di-photon system
$\Delta\phi_{\gamma\gamma}$ and $\Delta R_{\gamma\gamma}$	Azimuthal angular distance and ΔR between the two photons
Jet-related kinematic variables	
$m_{b\bar{b}}$, $p_{\mathrm{T}}^{b\bar{b}}$ and $y_{b\bar{b}}$	Invariant mass, transverse momentum and rapidity of the b-tagged jets system
$\Delta\phi_{b\bar{b}}$ and $\Delta R_{b\bar{b}}$	Azimuthal angular distance and ΔR between the two b-tagged jets
N_{jets} and $N_{b-\mathrm{jets}}$	Number of jets and number of b-tagged jets
H_{T}	Scalar sum of the p_{T} of the jets in the event
Photons and jets-related kinematic variables	
$m_{b\bar{b}\gamma\gamma}$	Invariant mass built with the di-photon and b-tagged jets system
$\Delta y_{\gamma\gamma,b\bar{b}}$, $\Delta\phi_{\gamma\gamma,b\bar{b}}$ and $\Delta R_{\gamma\gamma,b\bar{b}}$	Distance in rapidity, azimuthal angle and ΔR between the di-photon and the b-tagged jets system

ATLAS-CONF-2021-016

Search for $HH \rightarrow bb\gamma\gamma$: Systematic Breakdown

		Relative impact of the systematic uncertainties in %	
Source	Type	Non-resonant analysis HH	Resonant analysis $m_X = 300$ GeV
Experimental			
Photon energy scale	Norm.+Shape	5.2	2.7
Photon energy resolution	Norm.+Shape	1.8	1.6
Flavor tagging	Normalization	0.5	< 0.5
Theoretical			
Heavy flavor content	Normalization	1.5	< 0.5
Higgs boson mass	Norm.+Shape	1.8	< 0.5
PDF+α_S	Normalization	0.7	< 0.5
Spurious signal	Normalization	5.5	5.4

ATLAS-CONF-2021-016

VBF $H \to bb$: Adversarial Neural Network - selection

	Forward Channel Event Selection
b_1	≥ 1 b-tagged jet at 77% efficiency working point with $p_T > 85$ GeV and $\|\eta\| < 2.5$
b_2	≥ 1 b-tagged jet at 85% efficiency working point with $p_T > 65$ GeV and $\|\eta\| < 2.5$
j_1	≥ 1 jet with $p_T > 60$ GeV and $3.2 < \|\eta\| < 4.5$
j_2	≥ 1 jet with $p_T > 30$ GeV and $\|\eta\| < 4.5$
	$p_{T,bb} > 150$ GeV
	Central Channel Event Selection
b_1,b_2	≥ 2 b-tagged jets at 77% efficiency working point with $p_T > 65$ GeV and $\|\eta\| < 2.5$
j_1	≥ 1 jet with $p_T > 160$ GeV and $\|\eta\| < 3.1$
j_2	≥ 1 jet with $p_T > 30$ GeV and $\|\eta\| < 4.5$
	no jets with $p_T > 60$ GeV and $3.2 < \|\eta\| < 4.5$
	$p_{T,bb} > 150$ GeV, $m_{jj} > 800$ GeV

arXiv:2011.08280

VBF $H \to bb$: Adversarial Neural Network - Systematic Breakdown

Uncertainty	$\sigma(\mu_{H\to b\bar{b}})$
Statistics	± 0.31
NR Background Bias	± 0.15
Embedded Z	± 0.05
Experimental	$+0.10/-0.05$
Trigger	$+0.07/-0.03$
Jet	$+0.06/-0.04$
Flavor Tagging	$+0.02/-0.01$
Other	$+0.02/-0.01$
Signal Theory	$+0.06/-0.03$

arXiv:2011.08280

VBF $H \rightarrow bb$: With an additional photon selection

Trigger	L1	≥ 1 photon with $E_T > 22\,\text{GeV}$
	HLT	≥ 1 photon with $E_T > 25\,\text{GeV}$
		≥ 4 jets (or ≥ 3 jets and ≥ 1 b-jet) with $E_T > 35\,\text{GeV}$ and $\|\eta\| < 4.9$
		$m_{jj} > 700\,\text{GeV}$
Offline		≥ 1 photon with $E_T > 30\,\text{GeV}$ and $\|\eta\| < 1.37$ or $1.52 < \|\eta\| < 2.37$
		≥ 2 b-jets with $p_T > 40\,\text{GeV}$ and $\|\eta\| < 2.5$
		≥ 2 jets with $p_T > 40\,\text{GeV}$ and $\|\eta\| < 4.5$
		$m_{jj} > 800\,\text{GeV}$
		$p_T(b\bar{b}) > 60\,\text{GeV}$
		No electrons ($p_T > 25\,\text{GeV}, \|\eta\| < 2.47$) or muons ($p_T > 25\,\text{GeV}, \|\eta\| < 2.5$)

arXiv:2010.13651

VBF $H \to bb$: With an additional photon systematic breakdown

Source of absolute uncertainty	$\sigma(\mu_H)$ down	$\sigma(\mu_H)$ up
Statistical		
Data statistical	-0.78	$+0.80$
Bkg. fit shapes	-0.19	$+0.22$
Bkg. fit normalizations	-0.51	$+0.52$
Z boson normalizations	-0.15	$+0.14$
Systematic		
Spurious signal	-0.24	$+0.21$
Theoretical	-0.01	$+0.08$
Photon	-0.01	$+0.03$
Jet	-0.06	$+0.20$
b-tagging	-0.02	$+0.11$
Auxiliary	-0.01	$+0.04$
Total	-0.99	$+1.04$
Total statistical	-0.96	$+0.99$
Total systematic	-0.25	$+0.32$

arXiv:2010.13651

Search for heavy resonances decaying to a pair of photons: systematic breakdown

Signal yield			
Luminosity	±1.7%	Trigger	±0.5%
Photon identification	±0.5%	Photon isolation	±1.5%
Photon energy scale/resolution	negligible	Pile-up reweighting*	±(2–0.2)%
Spin-0 production process*	±(7–3)%		
*Signal modelling**			
Photon energy resolution	$^{+14\%}_{-9.3\%} - ^{+51\%}_{-29\%}$		
Photon energy scale	±(0.5–0.6)%		
Pile-up reweighting	negligible		
*Spurious signal, Spin-0**			
NWA	114–0.04 events (m_X = 160–2800 GeV)		
$\Gamma_X/m_X = 2\%$	107–0.14 events (m_X = 400–2800 GeV)		
$\Gamma_X/m_X = 6\%$	223–0.38 events (m_X = 400–2800 GeV)		
$\Gamma_X/m_X = 10\%$	437–0.50 events (m_X = 400–2800 GeV)		
*Spurious signal, Spin-2**			
$k/\overline{M}_{\rm Pl} = 0.01$	4.71–0.04 events (m_{G^*} = 500–2800 GeV)		
$k/\overline{M}_{\rm Pl} = 0.05$	19.0–0.09 events (m_{G^*} = 500–2800 GeV)		
$k/\overline{M}_{\rm Pl} = 0.1$	31.2–0.20 events (m_{G^*} = 500–2800 GeV)		

* mass-dependent

arXiv:2102.13405

Search for heavy resonances decaying to a pair of photons: limit summary

Spin-0		
m_X	400 GeV	2800 GeV
NWA	1.1 fb	0.03 fb
$\Gamma_X/m_X = 2\%$	2.5 fb	0.03 fb
$\Gamma_X/m_X = 6\%$	4.4 fb	0.03 fb
$\Gamma_X/m_X = 10\%$	8.3 fb	0.04 fb
Spin-2		
m_{G^*}	500 GeV	5000 GeV
$k/\overline{M}_{\mathrm{Pl}} = 0.01$	1.9 fb	0.04 fb
$k/\overline{M}_{\mathrm{Pl}} = 0.05$	2.3 fb	0.04 fb
$k/\overline{M}_{\mathrm{Pl}} = 0.1$	3.2 fb	0.04 fb

arXiv:2102.13405